126 (1979); M. Cloos, *Tectonics* **4**, 421 (1985).

46. J. P. Platt, *Geol. Soc. Am. Bull.* **86**, 1337 (1975); S. S. Sorensen, *Geol. Soc. Am. Mem.* **164**, 59 (1986); ——— and M. D. Barton, *Geology* **15**, 115 (1987); S. S. Sorensen, *J. Metamorph. Geol.* **6**, 405 (1988).
47. G. E. Bebout and M. D. Barton, *Geology* **17**, 976 (1989).
48. S. M. Peacock and P. J. Norris, *J. Metamorph. Geol.* **7**, 191 (1989).
49. E. Knoebl and S. M. Peacock, *Geol. Soc. Am. Abstr. Prog.* **21**, A276 (1989).
50. Calculated using the thermodynamic data of R. G. Berman [*J. Petrol.* **29**, 445 (1988)] and the GEOCALC program of T. H. Brown, R. G. Berman, E. H. Perkins [*Comput. Geosci.* **14**, 279 (1988)].
51. See, for example, K. Yamamoto and S. Akimoto, *Am. J. Sci.* **277**, 288 (1977).
52. A. L. Boettcher and P. J. Wyllie, *J. Geol.* **76**, 314 (1968); W. Johannes and D. Puhan, *Contrib. Mineral. Petrol.* **31**, 28 (1971); W. D. Carlson and J. L. Rosenfeld, *J. Geol.* **89**, 615 (1981).
53. F. S. Spear, *Am. J. Sci.* **281**, 697 (1981); J. G. Liou, S. Maruyama, M. Cho, *Mineral. Mag.* **49**, 321 (1985).
54. See, for example, articles in B. W. Evans and E. H. Brown, Eds., *Geol. Soc. Am. Mem.* **164**, (1986).
55. C. B. Raleigh and M. S. Paterson, *J. Geophys. Res.* **70**, 3965 (1965).
56. C. B. Raleigh, *Geophys. J. R. Astron. Soc.* **14**, 113 (1967); C. Meade and R. Jeanloz, *Eos* **70**, 1321 (1989).
57. Fluid infiltration can drive devolatilization reactions. The P-T stability field of a hydrous mineral is greatest in the presence of a pure H_2O fluid. Diluting the fluid phase with a component such as CO_2 reduces the stability field of a hydrous mineral. Thus, infiltration of a CO_2-bearing fluid into a rock can drive dehydration reactions; conversely, infiltration of H_2O-rich fluids can drive decarbonation reactions.
58. S. M. Peacock, *Geology* **15**, 1057 (1987).
59. P. Fryer, E. L. Ambos, D. M. Hussong, *Geology* **13**, 774 (1985).
60. S. M. Peacock, *Contrib. Mineral. Petrol.* **95**, 55 (1987).
61. See, for example, Y. Tatsumi, *J. Geophys. Res.* **94**, 4697 (1989).
62. J. D. Morris and S. R. Hart, *Geochim. Cosmochim. Acta* **47**, 2015 (1983); R. K. O'Nions, *Phil. Trans. R. Soc. London* **A310**, 591 (1984); W. M. White and P. J. Patchett, *Earth Planet. Sci. Lett.* **67**, 167 (1984); G. Faure, *Principles of Isotope Geology* (Wiley, New York, ed. 2, 1986); R. W. Kay, *ibid.*, p. 535. Island arc volcanic rocks from the South Sandwich Islands and the Lesser Antilles are enriched in radiogenic ^{87}Sr relative to mantle Sr; these data suggest that altered oceanic crust is contributing to arc magmas [C. J. Hawkesworth, R. K. O'Nions, R. J. Pankhurst, P. J. Hamilton, N. M. Evensen, *Earth Planet. Sci. Lett.* **36**, 253 (1977); C. J. Hawkesworth, R. K. O'Nions, R. J. Arculus, *ibid.* **45**, 237 (1979); J. P. Davidson, *Geochim. Cosmochim. Acta* **51**, 2185 (1987)]. Volcanic rocks from the Banda island arc (Indonesia) have Nd-Sr systematics that strongly suggest contamination by subducted terrigenous sediment derived from old continental crust [D. J. Whitford, W. M. White, P. A. Jezek, *Geochim. Cosmochim. Acta* **45**, 989 (1981)].
63. Created in the upper atmosphere, ^{10}Be is transported to the Earth's surface by precipitation where it partitions strongly onto soil and sediment. ^{10}Be concentrations are $>10^3$ times as great in pelagic sediments as in mid-ocean ridge and oceanic island basalts. Significantly elevated ^{10}Be concentrations have been found in lavas from the Japan, Aleutian, and Central American arcs, but not in lavas from the Mariana and Halmahera arcs. The 1.5 million year half-life of ^{10}Be demands relatively rapid (<10 million years) recycling of sediments in subduction zones in order to account for the elevated ^{10}Be concentrations in arc lavas. F. Yiou and G. M. Raisbeck, *Phys. Rev. Lett.* **29**, 372 (1972); S. Tanaka and T. Inove, *Earth Planet. Sci. Lett.* **49**, 34 (1980); L. Brown *et al.*, *Nature* **299**, 718 (1982); F. Tera, L. Brown, J. Morris, I. S. Sacks, *Geochim. Cosmochim. Acta* **50**, 535 (1986); J. D. Morris, W. P. Leeman, F. Tera, *Nature* **344**, 31 (1990).
64. C. R. Stern and P. J. Wyllie, *Am. Mineral.* **63**, 641 (1978); T. Sekine, P. J. Wyllie, D. R. Baker, *ibid.* **66**, 938 (1981).
65. Dry solidus, hornblende-out curve is from T. H. Green, in *Andesites*, R. S. Thorpe, Ed. (Wiley, New York, 1982), pp. 465–487; wet solidus is from I. B. Lambert and P. J. Wyllie, *J. Geol.* **82**, 88 (1972).
66. See, for example, Y. Hariya and S. Terada, *Earth Planet. Sci. Lett.* **18**, 72 (1973); M. C. Gilbert, T. H. Rosalind, R. K. Popp, F. S. Spear, in *Amphiboles: Petrology and Experimental Phase Relations*, D. R. Veblen and P. H. Ribbe, Eds. (*Rev. Mineral.* **9B**, Mineralogical Society of America, Washington, DC, 1982), pp. 229–353.
67. Dry solidus, E. Takahashi and I. Kushiro, *Am. Mineral.* **68**, 859 (1983); wet solidus, B. O. Mysen and A. L. Boettcher, *J. Petrol.* **16**, 520 (1975); hornblende out, D. H. Green, *Earth Planet. Sci. Lett.* **19**, 37 (1973); phlogopite out: R. F. Wendlendt and D. H. Eggler, *Am. J. Sci.* **280**, 385 (1980).
68. $MgO-SiO_2-H_2O$ phases are from (*51*); S. Kitahara, S. Takenouchi, G. C. Kennedy, *Am. J. Sci.* **264**, 223 (1966).

69. I thank G. E. Bebout, M. Cloos, W. G. Ernst, J. Holloway, and J. Tyburczy for helpful discussions regarding fluids in subduction zones. This work was supported by National Science Foundation grant EAR-8720343.

Mantle Oxidation State and Its Relationship to Tectonic Environment and Fluid Speciation

BERNARD J. WOOD, L. TARAS BRYNDZIA, KATHLEEN E. JOHNSON

The earth's mantle is degassed along mid-ocean ridges, while rehydration and possibly recarbonation occurs at subduction zones. These processes and the speciation of C-H-O fluids in the mantle are related to the oxidation state of mantle peridotite. Peridotite xenoliths from continental localities exhibit an oxygen fugacity (f_{O_2}) range from −1.5 to +1.5 log units relative to the FMQ (fayalite-magnetite-quartz) buffer. The lowest values are from zones of continental extension. Highly oxidized xenoliths (f_{O_2} greater than FMQ) come from regions of recent or active subduction (for example, Ichinomegata, Japan), are commonly amphibole-bearing, and show trace element and isotopic evidence of fluid-rock interaction. Peridotites from ocean ridges are reduced and have an average f_{O_2} of about −0.9 log units relative to FMQ, virtually coincident with values obtained from mid-ocean ridge basalt (MORB) glasses. These data are further evidence of the genetic link between MORB liquids and residual peridotite and indicate that the asthenosphere, although reducing, has CO_2 and H_2O as its major fluid species. Incorporation of oxidized material from subduction zones into the continental lithosphere produces xenoliths that have both asthenospheric and subduction signatures. Fluids in the lithosphere are also dominated by CO_2 and H_2O, and native C is generally unstable. Although the occurrence of native C (diamond) in deep-seated garnetiferous xenoliths and kimberlites does not require reducing conditions, calculations indicate that high Fe^{3+} contents are stabilized in the garnet structure and that f_{O_2} decreases with increasing depth.

THE MANTLE, REPRESENTING THAT VOLUME OF THE EARTH below the crust (10 to 40 km) and above the core (at 3200 km depth), may be presumed to have oxidation states ranging from equilibrium with Fe metal at the core-mantle boundary up to equilibrium with Fe^{3+}-rich silicate melts in the near-surface region. In this range, most major elements (for example, Si, Al, Mg, O, Ca, Na, Ti) have only one stable oxidation state, so that oxidation-reduction processes do not influence their geochemical behavior. One major element, Fe, and many minor elements such as C, S, Ni, Co, and V do, however, exhibit two or more stable oxidation states, and it is the distribution and behavior of these elements that holds the answers to many important questions about geological processes and the evolution of the earth. One would like to know, for example, whether the core and the mantle were ever in chemical equilibrium with one another and whether the mantle is undergoing secular changes in oxidation state. Because the earth is continuously degassing species of C, S, and H, the oxidation states of these elements and the overall degassing history of the mantle is inextricably linked to changes in the oxidation state of Fe.

Cycling of altered oceanic crust back to the mantle at subduction zones indicates that these zones are sources of secular hydration and oxidation. At mid-ocean ridges, on the other hand, peridotitic upper mantle partially melts to produce basalt, which rises, leaving a residue in which the proportions of Fe^{3+}-bearing phases such as spinel and of hydrous phases such as amphibole and of carbonates are greatly diminished. Mid-ocean ridges appear, therefore, to be zones of potential dehydration, decarbonation, and reduction. More detailed evaluation of the processes involved requires careful characterization of mantle rocks and of mantle-derived products such as lavas and magmatic gases from as wide a range of tectonic and geographic environments as possible. Mantle samples available for study include peridotitic and eclogitic xenoliths entrained in alkali basalts and kimberlites from both continental and oceanic regions. Diamond xenocrysts in kimberlites contain silicate, sulfide, and other inclusions and provide evidence of the stability of native C in the deep continental lithosphere. Larger scale peridotite bodies intruded into the continental crust provide us with the opportunity to investigate small scale variations in oxidation state and the influence of melt intrusions (which are common in such bodies) on upper mantle properties.

Oxidation State, Oxygen Fugacity, and Fluids

In the earth, Fe occurs in the oxidation states Fe(O), Fe(II), and Fe(III), but Fe(II) is dominant in the peridotitic upper mantle. In pure end-member phases, these three oxidation states have well-defined stability fields in oxygen fugacity (f_{O_2})-pressure-temperature (P-T-f_{O_2}) space, and it is normal to compare the oxygen fugacities recorded by natural assemblages to the values of well-known end-member reactions. For example, we may consider the reactions:

QIF 2 Fe (metal) + SiO_2 (quartz) + O_2 = Fe_2SiO_4 (fayalite)
IW Fe (metal) + 1/2 O_2 = FeO (wustite)
WM 3 FeO (wustite) + 1/2 O_2 = Fe_3O_4 (magnetite)
FMQ 3 Fe_2SiO_4 (fayalite) + O_2
= 2 Fe_3O_4 (magnetite) + 3 SiO_2 (quartz)
MH 2 Fe_3O_4 (magnetite) + 1/2 O_2 = 3 Fe_2O_3 (hematite)

as defining planes of increasing f_{O_2} in P-T-f_{O_2} space (Fig. 1).

Similarly, the upper stability limit of C is defined by the CCO equilibria (Fig. 1):

$$C + 1/2\ O_2 = CO$$

$$C + O_2 = CO_2$$

where $p_{CO_2} + p_{CO} = 1$ atm (p, partial pressure). As can be seen in Fig. 1, the stability fields of Fe^{2+}-bearing assemblages are limited at 1 atm in these simple systems by the FMQ and QIF reactions; Fe(II) is thus stable over a total range in f_{O_2} of about 5 log units. In the mantle, however, the Fe^{2+} field is greatly expanded because of solid solution in magnesium-rich olivine and pyroxene. Thus, the fact that Fe(II) is the dominant oxidation state in the upper mantle does not closely constrain f_{O_2}. At 1 atm the upper stability limit of C is in the stability field of Fe metal, and at first glance this might imply that the presence of native C in some xenoliths (*1, 2*) requires compatibility with the metal. In practice, however, the stability field of C is strongly pressure-dependent at low pressure so that at 15 kbar it is close to the FMQ curve (Fig. 2). Thus, native C is actually compatible with a wide range of mantle oxygen fugacities.

In that graphite or diamond is stable over a wide range of f_{O_2}, the compositions of mantle fluids, if present, may vary widely, too. Because hydrous phases are quite common in upper mantle rocks and H_2O is a dominant component in many volcanic gases (*3*), C-H-O fluid species are of greatest importance in mantle fluids.

To illustrate the relations between f_{O_2} and fluid composition, Fig. 2 has been contoured in mole fraction of CH_4 in an equilibrium C-H-O fluid coexisting with graphite under the P-T-f_{O_2} conditions of interest. In the stability field of Fe, below IW, the fluid is greater than 80% methane, whereas at the upper stability limit of C the fluid is essentially all CO_2. In between these two extremes lies a region in which H_2O-rich fluids dominate, as illustrated in Fig. 3. Thus, the major element compositions of fluids involved in mantle processes are strongly dependent on f_{O_2}, which in turn affects the nature of melting products (*4*) and the solubilities of transportable species such as Si, alkalies and rare earth elements (REE) (*5*).

Measurement of Mantle f_{O_2}

Some indication of the redox properties of the mantle are provided by the compositions of lavas that have their source regions at depth. For example, many basalts from both continental and oceanic areas contain two coexisting iron-titanium oxide solid solutions (Fe_2O_3-$FeTiO_3$ and Fe_3O_4-Fe_2TiO_4), the compositions of which yield both f_{O_2} and temperature of equilibration (*6*). Haggerty (*7*) has used this approach to show that both subaerial and suboceanic basalts generally yield f_{O_2} values close to FMQ. More

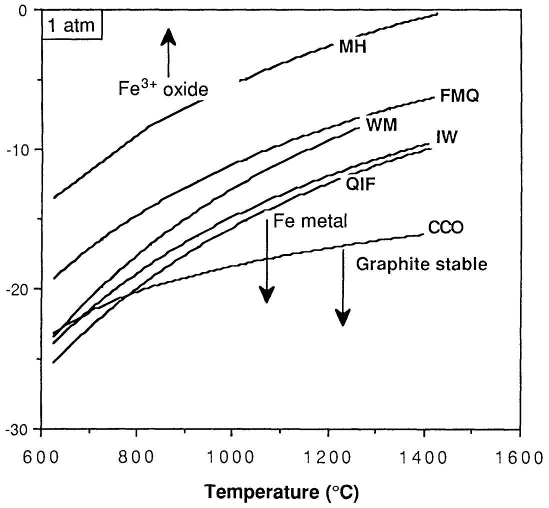

Fig. 1. Oxygen fugacity-temperature relations for reactions involving Fe(O), Fe(II), Fe(III) and C at 1 atm total pressure; Fe_2O_3 is stable above MH and Fe^0 metal below IW in absence of silicates or below QIF if SiO_2 is present. Field between IW and MH is that of various Fe(II)-Fe(III) equilibria (see text). Native C is only stable in the Fe (metal) field at high temperatures.

B. J. Wood is in the Department of Geology, University of Bristol, Bristol BS8 1RJ United Kingdom. L. T. Bryndzia and K. E. Johnson are in the Department of Geological Sciences, Northwestern University, Evanston, IL 60208.

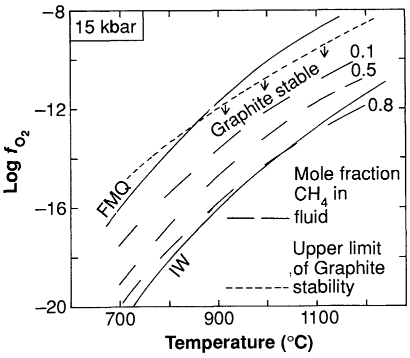

Fig. 2. The region between FMQ and IW of Fig. 1 recalculated at 15 kbar. Graphite is stable to much higher f_{O_2} than at 1 atm. Labeled contours refer to calculated mole fractions of CH_4 in equilibrium C-H-O fluids. At the upper limit of graphite stability the fluid is essentially pure CO_2 (Fig. 3). Below IW the fluid is 80% CH_4.

recent data demonstrate, however, that these conditions may not apply to the mantle source region of the basalts because degassing of the melt at, or near, the surface can effect rapid changes in oxidation state and f_{O_2}.

Christie *et al.* (*8*) determined the Fe^{3+}/Fe^{2+} ratio of glasses from mid-ocean ridge pillow lavas and applied an experimental calibration of the f_{O_2} dependence of Fe^{3+}/Fe^{2+} ratios in liquids (*9*) in order to calculate the apparent oxygen fugacities of the quenched melts. These data showed that the whole rocks and cores of the pillows (Fig. 4) were more oxidized than the rapidly quenched glassy rims. The implication is that degassing of the more slowly cooled centers, possibly by loss of H_2, caused significant shifts in f_{O_2} to values near or above FMQ (Fig. 4), whereas the pillow rims recorded oxidation states closer to the initial undegassed state. These authors suggested that the glass values, which average about −1.3 log units in f_{O_2} relative to FMQ at 1 atm and 1200°C represent an upper bound on values in the mantle source region, but measurements on actual mantle samples are clearly required.

Most mantle xenoliths in basaltic and kimberlitic magmas are peridotite, consisting of olivine and orthopyroxene with minor amounts of clinopyroxene, and spinel or garnet. Hydrous phases, mainly phlogopite and amphibole, occur in a few samples. The combination of olivine (~70%) and the other anhydrous phases appears, from frequency of occurrence and correspondence with measured elastic properties to dominate the mantle to a depth of at least 400 km (*10*).

Attempts to measure the oxygen fugacities recorded by spinel peridotites and ilmenite megacrysts electrochemically (*11*) revealed values that spanned almost the entire range of stability of Fe^{2+}-bearing silicates, from below IW to above FMQ. Most likely, however, the highly reduced values are an artifact of the experimental method, which involved measurement at 1 atm under anhydrous conditions. Many xenoliths contain small amounts of reduced C on surfaces and in cracks (*1*) and, although stable over a wide range of f_{O_2} at high pressures (Fig. 2), this material is only stable below IW at 1 atm (Fig. 1). Virgo *et al.* (*12*) have thoroughly documented the reduction of Fe^{3+} to Fe^{2+} caused by such C during electrochemical measurements on ilmenite megacrysts. The effect is to shift the apparent f_{O_2} from the true value down toward the CCO line of Fig. 1. The sample acquires a lower Fe^{3+}/Fe^{2+} ratio than was originally present, and once all of the C has been reacted out, will give an apparent low f_{O_2}, which, in T-f_{O_2} space, subparallels the IW buffer curve. Thus, although correct values can be obtained if C is completely absent, the highly reduced values found in some studies are unlikely to refer to the true mantle f_{O_2}. This assertion is corroborated by the observation that upper mantle olivine contains too much Ni for it to be in equilibrium with Fe-rich metal. O'Neill and Wall (*13*) calculated the conditions under which olivine containing 2500 to 3500 ppm of Ni (typical for the upper mantle) would precipitate metal. Their calculation gives a lower bound on possible f_{O_2} that corresponds to conditions essentially at IW. Thus, f_{O_2} values below IW are precluded because Fe metal does not occur in upper mantle phases except as rare inclusions in diamond (*14*).

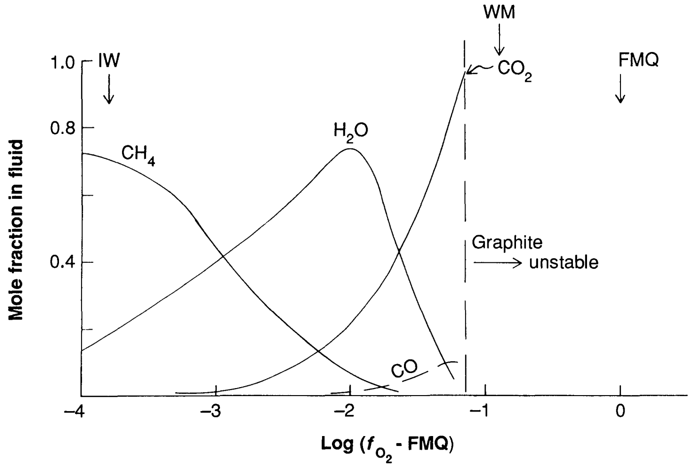

Fig. 3. Composition of C-H-O fluid in equilibrium with graphite at 10 kbar and 1127°C. Graphite is stable only if f_{O_2} is more than 1.2 log units below FMQ, under which conditions the fluid is almost pure CO_2. H_2O dominates at somewhat lower f_{O_2} while CH_4 is the major species close to IW.

Oxygen thermobarometry is the most promising method of determining f_{O_2} because it relies on properties of the minerals that cannot be rapidly reset during cooling or perturbed by normal measurement techniques. The approach relies on the observation that both ferrous and ferric components are present in the peridotite phases. For example, almost all spinel peridotites contain the assemblage olivine-orthopyroxene-spinel, and apparent f_{O_2} may be determined from the equilibrium (opx, orthopyroxene):

$$\underset{\text{olivine}}{6\,Fe_2SiO_4} + O_2 = \underset{\text{opx}}{6\,FeSiO_3} + \underset{\text{spinel}}{2\,Fe_3O_4} \qquad (1)$$

Determination involves measuring the concentrations of Fe_2SiO_4, $FeSiO_3$, and Fe_3O_4 components in the olivine, orthopyroxene, and spinel phases, respectively, and calculating f_{O_2} from thermodynamic data on the end-member reactions with the use of activity-composition relations for the complex phases.

Although in theory this method should yield values with overall uncertainty of ±0.2 log units in f_{O_2}, the values can have a bias because of errors in the determination of Fe^{3+} contents (and hence Fe_3O_4 contents) of spinel and because of uncertainties in the activity-composition relations of spinel (*13, 15, 16*). The Fe_2SiO_4 and $FeSiO_3$ contents of olivine and orthopyroxene, respectively, can be readily determined by electron microprobe. Upper mantle phases typically contain about 0.1 mole fraction of these iron end-members. Almost all of the remaining 0.9 mole fraction consists of the analogous Mg components. Microprobe determination of Fe^{3+} in spinel hinges, however, on the assumption that this phase maintains perfect M_3O_4 stoichiometry in the f_{O_2} range of concern. Thus, total Fe is determined as FeO and the proportion of Fe^{3+} is estimated by conversion of Fe^{2+} to Fe^{3+} until the cation:oxygen ratio becomes 3:4. The small uncertainties in the atomic-number, absorption, and fluorescence correction factors in the microprobe measurements of the light elements, Mg and Al, that are present at high concentration in these spinels, become magnified and result in large fractional errors in the calculated Fe^{3+} content because this represents only about 1% by weight of the mineral (*16*). In contrast to systematic errors, the precision of the microprobe method is good (standard deviation of about ±0.002 mole fraction Fe_3O_4), and thus, with careful calibration, such analyses could be used for thermobarometry.

Fig. 4. Oxygen fugacities of MORB glasses and whole rocks from the Mid-Atlantic Ridge as determined by homogeneous Fe^{2+}-Fe^{3+} equilibrium in silicate melt (*8*). Rapidly quenched glasses from pillow margins are more reduced than whole rocks and pillow cores, possibly because of H_2 loss from the cores during slower cooling.

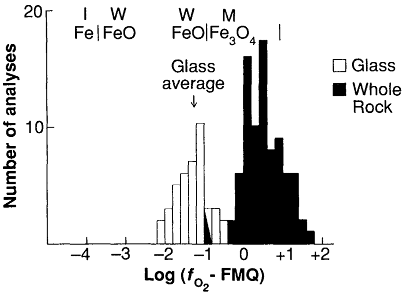

In order to reduce the analytical uncertainty, Wood and Virgo (*16*) separated spinels from 30 continental spinel lherzolite xenoliths and determined their ferric/ferrous ratios by Mössbauer spectroscopy, a technique that has an uncertainty of about ±10% relative when used to measure typical ferric-to-total iron values of between 0.15 and 0.3. The spectroscopic method greatly reduces systematic errors in measured Fe^{3+}/Fe^{2+} ratios and yields a range of Fe_3O_4 contents of between 1.7 and 5.2 mole percent. It was also shown that the use of Mössbauer-analyzed spinels as microprobe standards enables the uncertainty in the probe method to approach its precision.

Estimation of activity-composition relations for spinel is difficult because of Fe^{2+}-Fe^{3+} disorder between octahedral and tetrahedral sites in the structure. Nevertheless there have been several recent experimental and theoretical attempts to predict the activity of Fe_3O_4 component in spinel at the low concentration conditions (0 to 5 mole percent Fe_3O_4) of interest (*13, 15*). Because these studies obtained similar results, we have made a direct experimental test of the uncertainty in the calibrated thermobarometer of Reaction 1. The test involved mixing together natural olivine, natural orthopyroxene and a number of different synthetic and natural spinels. The spinels mimicked mantle compositions in that $MgAl_2O_4$ was dominant (0.45 to 0.825 mole fraction), they had a wide range of $FeCr_2O_4$ contents (0.125 to 0.50 mole fraction) and Fe_3O_4 was present in the 0 to 5 mole percent range. Reversal experiments were made at 1200°C and 1 atm total pressure with spinels that had low and high initial Fe_3O_4 contents and with f_{O_2} controlled at between FMQ and about 1.3 log units below FMQ. After the experiment (of 5 to 7 days duration) the samples were quenched, products analyzed by microprobe and apparent equilibration oxygen fugacities were calculated from three of the current versions of the thermobarometer. These calculated values are compared with the actual experimental ones in Fig. 5.

All three versions of the thermobarometer gave good results and thus can be used, with some caution, to obtain accurate estimates of f_{O_2} recorded by the spinel-olivine-orthopyroxene assemblage. The Mattioli-Wood (*15*) version, which was experimentally calibrated for Cr-free spinels, gives results that, not surprisingly, depend slightly on Cr/Cr+Al ratio. Thus, although the average f_{O_2} is close to the true value (within 0.2 log units), spurious correlations of f_{O_2} with Cr-content of the spinel are possible. The O'Neill-Wall (*13*) version, based on an elaborate order-disorder model and a range of experimental data on simple and complex spinels, shows no composition dependence. It does, however, appear to underestimate f_{O_2} slightly (about 0.6 log units). Finally, the Nell-Wood (*17*) version incorporates the data sets of the earlier versions and contains a large number of new measurements of cation disorder. This version has no apparent composition dependence and yields good agreement (within 0.3 log units average) between calculated and actual, experimental f_{O_2}. Thus, it appears that oxygen thermobarometry is sufficiently well developed to permit reliable application to spinel peridotites (*18*).

At depths greater than about 60 km spinel breaks down to yield garnet in reactions such as

spinel + orthopyroxene + clinopyroxene → garnet + olivine

This means that equilibria other than Reaction 1 need to be calibrated in order to estimate f_{O_2} for the garnetiferous assemblages of the deeper parts of the continental lithosphere. Recent Mössbauer measurements (*19*) demonstrate that the garnet phase contains significant amounts of Fe^{3+} (ratios of molar Fe^{3+} to total Fe of up to 0.17) and that this iron resides in octahedral coordination in the garnet structure. Thus, potential thermobarometers for the garnet assemblage could include

$$\underset{\text{clinopyroxene}}{3\,CaFeSi_2O_6} + \underset{\text{olivine}}{2\,Fe_2SiO_4} + 1/2\,O_2 = \underset{\text{garnet}}{Ca_3Fe_2^{3+}Si_3O_{12}} + \underset{\text{opx}}{5\,FeSiO_3} \quad (2)$$

or

$$\underset{\text{olivine}}{2\,Fe_2SiO_4} + \underset{\text{opx}}{FeSiO_3} + 1/2\,O_2 = \underset{\text{garnet}}{Fe_3^{2+}Fe_2^{3+}Si_3O_{12}} \quad (3)$$

However, because of current uncertainties in the end-member and mixing properties of the garnet components, the garnet-peridotite data can be used for little other than to infer that oxygen fugacities are probably within about 2 log units of FMQ and that ferric iron may affect calculated temperatures of equilibration (*19*). Thus, most of the remainder of the discussion centers on the spinel-peridotite facies of the upper mantle, although experimental calibration of redox equilibria involving garnet is clearly essential to the understanding of the oxidation state of the deeper continental lithosphere.

Oxygen Barometry of Continental Spinel Lherzolite Xenoliths

Continental spinel lherzolite xenoliths are fresh samples of the subcontinental lithosphere brought up from between 30 and 60 km depth by alkali basalt volcanism. They contain olivine, orthopyroxene, clinopyroxene, and spinel and are thus appropriate for oxygen thermobarometry. Figure 6 shows calculated oxygen fugacities of the 30 continental spinel lherzolites for which Mössbauer data were obtained by Wood and Virgo (*16*). The figure is slightly different from the two given in (*16*) because f_{O_2} calculations are now made with the Nell-Wood model, which has no apparent compositional bias. Temperatures recorded by these continental xenoliths, as obtained from the Wells (*20*) two-pyroxene geothermometer, range from 914° to 1095°C. In order to facilitate comparison among the data, we have referenced all analyses to the FMQ curve, because temperature errors of ±100°C only shift relative f_{O_2} by ±0.2 log units when it is normalized in this fashion. In the absence of an accurate geobarometer for spinel lherzolite assemblages we performed the calculation at a pressure of 15 kbar, essentially in the middle of the spinel field (*21*). As with temperature, f_{O_2} relative to FMQ is little affected by pressure errors within the stability field of spinel lherzolite.

Several important features may be observed from the data (Fig. 6). Firstly, it is of interest to compare the data with oxygen barometry on the rapidly quenched MORB glasses (*8*). In comparison with the 1-bar data, most continental xenoliths lie outside the MORB range. The effect of pressure on ferric-ferrous equilibria in silicate liquids is poorly known, but if the liquid partial molar volume data for Fe_2O_3 and FeO of Lange and Carmichael (*22*) are used, then the MORB liquids would lie at higher f_{O_2} (relative to FMQ) at high pressure than at 1 bar (Fig. 6). For purposes of comparison in Fig. 6, we used a pressure of 15 kbar for both MORB and peridotites, although the actual pressure of MORB generation probably varies substantially. Even if this type of pressure correction is applied, most of the continental xenoliths are more oxidized than the most oxidized MORB glass. Therefore, a large part of the continental lithosphere, although of similar composition, is distinct from the MORB source region.

A second important feature of Fig. 6 is that all of the samples from Ichinomegata, Japan, and from Mont Briancon in the Massif Central of France lie above FMQ and are outside the range of MORB glasses. All of the Japanese samples contain amphibole or the remnants of amphibole that have undergone decompression melting. Furthermore, this locality lies above the subducting Pacific plate, and xenoliths containing H_2O-bearing fluid inclusions have been reported (*23*). These data strongly imply that the subduction environment is one where the mantle overlying the descending plate undergoes oxidation in addition to hydration. In support of a correlation between oxidation and hydration, data on five amphibole-bearing xenoliths from the Eifel region (currently a rift environment, but in an area of subduction in the past) of Germany also yielded f_{O_2} values above FMQ. The Mont Briancon oxidized samples, although apparently anhydrous, are also from a region of subduction in the recent geologic past. Mattioli *et al.* (*24*), using a large database of microprobe analyses, also noted that there was a correlation between hydrated and oxidized samples, and, despite the reservations over the use of microprobe data, the observed relations have held up when the spinels were analyzed by Mössbauer spectroscopy. Further geochemical evidence for interaction of the mantle with a slab-derived fluid component is apparent open-system oxygen isotope behavior of the hydrous Eifel samples (*25*) and the enrichment in oxidized samples of phlogopites in Ba and amphiboles in light rare earth elements (LREE), which are likely derived from the slab (*26*). We therefore concur with Mattioli *et al.* (*24*) in observing that amphibole-bearing samples are oxidized and enriched (commonly) in LREE and Ba, and that this process occurs above subduction zones. The agents of metasomatism are most probably hydrous melts and the fluids associated with melting and crystallization phenomena in the mantle wedge.

Continental xenoliths from Kilbourne Hole, San Carlos, and Central Asia are more reduced than those previously discussed and exhibit an f_{O_2} range from FMQ to about 1.5 log units below FMQ (that is, some are within the MORB range and some are above it). Because these localities are in regions of continental extension where the asthenosphere is relatively close to the surface, it is not surprising that some samples have affinities with MORB. Recent trace element and isotopic data (*27, 28*) have also shown that some of the San Carlos and Kilbourne Hole xenoliths have isotopic and LREE signatures characteristic of MORB-related mantle (that is, without LREE enrichment). Other xenoliths show evidence of LREE enrichment, but without any mineralogic manifestation of metasomatism.

In view of the correlation between high f_{O_2} values and trace

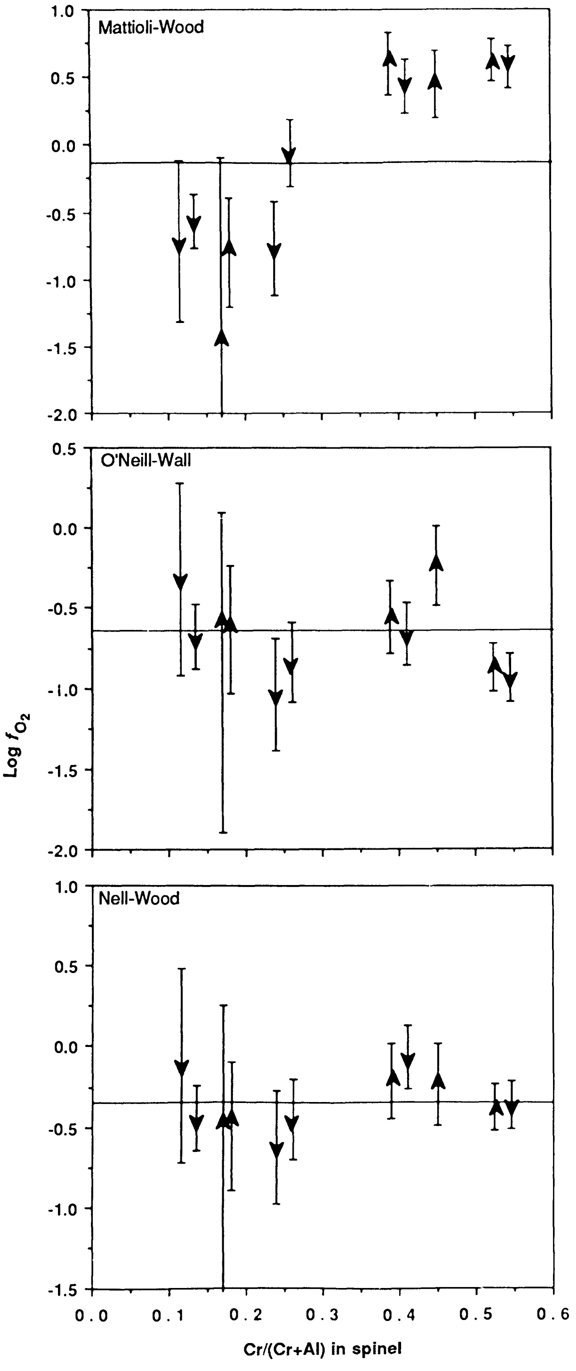

Fig. 5. Experimental tests of 3 different versions of the spinel peridotite oxygen barometer at 1 atm and 1200°C. Experiments were performed by re-equilibrating olivine, orthopyroxene, and spinel at known (experimental) f_{O_2}. Re-equilibrated phase compositions were then used to calculate apparent f_{O_2}. Error bars refer to ±1 SD or approximately ±4 SE. The Nell-Wood version (*18*) gives the best overall agreement, but all three yield petrologically useful results.

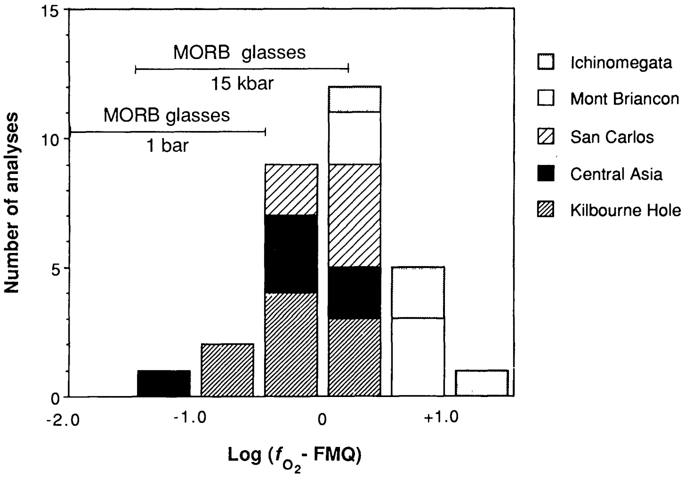

Fig. 6. Histogram of oxygen fugacities (relative to FMQ) obtained for continental spinel lherzolite xenoliths using the spinel peridotite barometer. Subduction zone xenoliths (Ichinomegata, Japan and Mont Briancon, France) are all above FMQ whereas regions of continental extension (San Carlos, Arizona; Kilbourne Hole, New Mexico; and Central Asia) show a range from MORB-like to oxidized.

element enrichments in the subduction environment, it is tempting to suggest that the samples enriched in trace elements in extensional environments also correspond to the more oxidized samples. We tested this suggestion by measuring REE and other lithophile-element contents of clinopyroxene separates from Kilbourne Hole and San Carlos specimens. Similar analyses were made on samples from Dish Hill, California, and from the Anakie Hills of Southeast Australia. Surprisingly, there was no correlation between trace element enrichment and f_{O_2} in these anhydrous specimens. Thus, although some of the samples from these extensional environments exhibit MORB-like oxygen fugacities and some have MORB-like isotopic and trace element signatures, the sample groupings are not coincident.

In summary, the extensional continental environment is one of local f_{O_2}, trace element, and isotopic heterogeneity caused by mixing of older continental lithosphere with younger asthenosphere. The lack of correlation between f_{O_2} and high trace element concentration probably reflects the ease with which f_{O_2} may be perturbed. Spinels constitute around 3% by volume of spinel lherzolites, and they contain about 1% Fe_2O_3 by weight. The f_{O_2} recorded by these rocks is thus not well buffered, and it may be perturbed by the infiltration of relatively small volumes of oxidizing or reducing fluid. A straightforward calculation reveals that infiltration of C-H-O fluids similar in composition to those shown in Fig. 3 can perturb f_{O_2} in these lherzolites by 2 log units at volumetric fluid/rock ratios of 0.01. Thus, we consider that in an environment with a long and complex history such as that of continental extension, small amounts of fluid associated with magmatism can decouple f_{O_2} from trace element signatures. The measured f_{O_2} in this environment, records a mixture of old and new (magmatism-related) signatures. The subduction environment is different because the spinels are much more oxidized (up to 6% Fe_2O_3), and the rocks contain other phases rich in ferric iron, notably amphibole. Mössbauer experiments on amphibole indicate that this phase typically has a Fe^{3+}/Fe^{2+} ratio about the same as that of the coexisting spinel, and it is modally much more abundant than the spinel. Thus, with a ratio of Fe^{3+} to total Fe between 0.3 and 0.4, these rocks have some buffering capacity and are much less readily altered than the more reduced samples from the extensional environment. At high f_{O_2}, therefore, correlations between LREE and other trace element enrichments and f_{O_2} are preserved whereas at low f_{O_2} they are readily perturbed.

Reference to Fig. 3 shows that almost all of the continental spinel peridotites crystallized at f_{O_2} values outside the field of graphite stability. Thus, fluids in equilibrium with them cannot contain reduced species like CO or CH_4 but must be mixtures of CO_2 and H_2O. At the pressures and temperatures of concern (10 to 15 kbar; 900° to 1200°C), the strong partitioning of H_2O into amphibole or melt leaves a CO_2-rich fluid. Because, with the exception of the Ichinomegata samples discussed above, almost all fluid inclusions in spinel peridotites are nearly pure CO_2 (*29*), there is good agreement between inferred and measured fluid compositions.

Suboceanic Peridotites

Abyssal peridotites have been dredged and drilled from a large number of fracture zones along the earth's mid-ocean ridge systems. These peridotites are generally hydrothermally altered, but by analysis of relict phases and determination of modes, primary rock and mineral compositions can be reconstructed (*30*). Furthermore, fresh unaltered spinel is quite common, enabling application of the spinel peridotite oxygen barometer. Dick *et al.* (*30*) have provided convincing chemical evidence that these abyssal peridotites are the residues of partial melting and that they are thus the residuum of the mantle from which MORBs were formed.

Oxygen thermobarometry of abyssal peridotites from mid-Atlantic, central Indian, southwest Indian, and American-Antarctica ocean ridge systems as well as the Cayman Trough (*31*) reveals that these rocks are substantially more reduced than the continental peridotites discussed earlier. Calculated values, with the Nell-Wood version of the thermobarometer (Fig. 7) and at an assumed pressure of 15 kbar, give an average f_{O_2} of −0.9 log units relative to FMQ, about 1 log unit below the average for continental spinel peridotites. This value is virtually coincident with the mean of the values for MORB glasses when the latter are corrected to 10 to 15 kbar. [The distribution of data is slightly different from that shown in (*31*) because of our use of the more recent Nell-Wood version of the geobarometer. The conclusions of Bryndzia *et al.* are not substantially altered by this change of calibration, however.] Even if we assume that the estimated pressure effect is too large, the MORB mean at 1 bar (−1.28 log units relative to FMQ) is essentially the same as that for the abyssal peridotites within uncertainty. The agreement between the two data sets solidifies the idea that there is a genetic link between the abyssal peridotites (residuum) and the MORB (melting products). Furthermore, the agreement with data for rapidly quenched MORB glasses from pillow margins suggests that the margins have not undergone significant degassing (hydrogen loss) during quenching. This is in contrast to the pillow cores, which are more oxidized (*8*), as shown above.

Four of the six most reduced abyssal peridotites shown in Fig. 7 came from the Islas Orcadas fracture zone, a region which produces "hotspot" or "plume" basalts and is close to the Bouvet Island hotspot of the southwest Indian Ridge (*30*). These four samples exhibit a range of f_{O_2} from −1.85 to −2.64 log units relative to FMQ, well below the average value of −0.9 log units. One possible interpretation is that mantle plumes are more reduced than normal asthenospheric mantle. An alternative explanation is that MORBs and their residues are fluid saturated during the melting process (*32*) and that the variations in f_{O_2} reflect an increasing extent of melting at hotspots relative to "normal" ridge. For example, Fig. 8 shows that, at fluid saturation (in the C-O system) and equilibrium with graphite, increasing degrees of melting (due to decompression or heating) would yield decreasing f_{O_2} relative to FMQ. The absolute values of f_{O_2} for fluid and graphite saturation in the MORB melting range (10 to 15 kbar; ~1350°C) (*33*) are also in approximate agreement with those observed. Thus, the simplest interpretation would be that MORB production takes place under fluid and

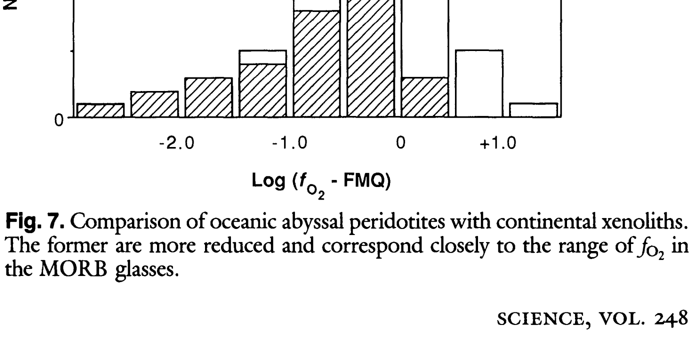

Fig. 7. Comparison of oceanic abyssal peridotites with continental xenoliths. The former are more reduced and correspond closely to the range of f_{O_2} in the MORB glasses.

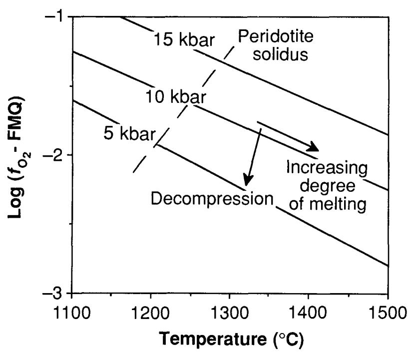

Fig. 8. Possible mechanisms by which increased degree of melting at a hotspot could yield progressively more reduced magmas. Assumptions are saturation in graphite and the presence of a C-O fluid. Peridotite solidus at high pressure (dashed line) from (*33*).

graphite saturated conditions and that variation in f_{O_2} in MORB and residual peridotite is primarily a result of differences in the pressure-temperature conditions of melting.

Several questions remain. Firstly, it will be necessary to sample more hotspot localities in order to test the observed relations in f_{O_2}. Secondly, the hypothesis of fluid saturation during melting relies on measurements of solubility of CO_2 (the dominant fluid species) in basaltic melts at high pressure coupled with estimates of the amount of CO_2 evolved during volcanism (*34*). The solubility measurements are highly uncertain at present (*35*). Although isotopic measurements of the $^{13}C/^{12}C$ ratio in C dissolved in basalt support the hypothesis of fluid saturation (*36*), this interpretation has also been disputed (*37*).

In summary, abyssal peridotites are more reduced than continental spinel peridotite xenoliths and their range in f_{O_2} is consistent with the notion that they are residua from MORB generation. The association of the most reduced samples with a hotspot locality suggests either that low f_{O_2} is a characteristic of the hotspot environment or that it reflects a larger than "normal" extent of melting under fluid-saturated conditions. Although more data are needed to clarify these observations, reference to Fig. 3 shows that any fluid produced during generation of MORB must, even at graphite saturation, be rich in CO_2 and poor in reduced species such as CO and CH_4. Under the most reduced f_{O_2} conditions, CH_4 contents are likely to be less than 20 mol percent at graphite saturation (Fig. 3).

Massif Peridotites

Peridotite massifs are large (kilometer-size) pieces of the upper mantle that become incorporated in the crust via diapiric upwelling and continental collision. As such they provide the opportunity for detailed study of the small scale variations in f_{O_2} and other geochemical parameters that may characterize the mantle. A preliminary study of the Ronda (Spain) and Beni Bousera (Morocco) massifs has been made by Woodland *et al.* (*38*). Both of these massifs contain textural, mineralogical and geochemical evidence suggesting that they rose from depths in the garnet lherzolite field (*39, 40*) and that the garnet broke down to form spinel en route to the surface. In the case of Beni Bousera, the presence of pseudomorphs of graphite replacing diamond (*41*) suggests that this massif had an origin at pressures of >50 kbar. The presence of veins and dikes in both massifs indicates that they have undergone partial melting (*42*). Initial measurements indicate that the two massifs have oxygen fugacities similar to those of abyssal peridotites and unlike those of the continental xenoliths. Furthermore, a range of greater than 2 log units in f_{O_2} is observed, and there is no systematic variation across the bodies. The spread in f_{O_2} values is similar to that in MORB glasses (Fig. 4), abyssal peridotites, and continental xenoliths (Fig. 6) and indicates that small-scale variations in oxidation state occur in the upper mantle.

The Ronda and Beni Bousera massifs appear, therefore, to be two examples of peridotites that originated in the asthenosphere and that have the f_{O_2} ranges characteristic of suboceanic mantle. They did not have their oxygen fugacities modified during their short residence times in the lithosphere. Whether other peridotite massifs have similar ranges of f_{O_2} is not yet known.

Garnet Facies of the Lithosphere and Asthenosphere

As discussed above, during the transition from spinel lherzolite to garnet lherzolite with increasing pressure, ferric iron enters the garnet phase in octahedral coordination (*19*), but experimental calibration of appropriate equilibria (reactions 2 and 3) have not been made. Currently available data suggest that the f_{O_2} of the garnet xenoliths is close to FMQ (*19*), but this cannot yet be regarded as a definitive result.

Garnet lherzolites, eclogites, and diamonds are all associated with kimberlitic intrusions of the continental cratons. The occurrence of diamond places an upper bound on f_{O_2} at values close to FMQ [(*43*) and Fig. 2]. Diamonds commonly contain inclusions of minerals analogous to those of the eclogitic and peridotitic suites of xenoliths (garnet, pyroxene, olivine, and so forth), and model Pb ages of these inclusions suggest that they are much older than the kimberlites themselves; the ages extend back to the Archean (*44*). Thus, measurement of the oxidation states of these inclusions should enable us to determine whether there has been secular variation in upper mantle f_{O_2}. In principle, studies of old volcanic products would also yield such information, but problems of degassing and alteration observed in modern lavas probably make any old signature virtually decipherable.

Although a more detailed study of garnet lherzolite xenoliths and of diamond inclusions will enable extension of the thermobarometric method to >150 km depth, the high densities of ferric garnets already suggest an interesting depth-f_{O_2} relation. If the f_{O_2} range exhibited in the spinel facies is preserved and if, at high pressures, ferric iron enters garnet without a significant break in f_{O_2} at the spinel-garnet boundary, the variation in f_{O_2} as a function of pressure in the garnet field is simply given by the volumes of products and reactants in reactions 2 and 3. Irrespective of whether reaction 2 or 3 is used, f_{O_2} should decrease relative to FMQ with depth in the garnet field. [For reaction 3 the volume (V) of $Fe_3^{2+}Fe_2^{3+}Si_3O_{12}$ was estimated from $V_{Fe_3Al_2Si_3O_{12}} + V_{Ca_3Fe_2^{3+}Si_3O_{12}} - V_{Ca_3Al_2Si_3O_{12}}$]. Thus, for the same range in ferric contents of the mantle in the garnet field as in the spinel field, f_{O_2} should decrease relative to FMQ with increasing depth in the garnet field, as shown in Fig. 9. We have made approximate calculations of equilibrium fluid compositions under these predicted f_{O_2} conditions using recent estimates of the high pressure fluid equations of state (*45*) (Fig. 9). Thus, the equilibrium C-H-O fluid should be CO_2-rich in the zone of basalt generation, become H_2O rich in the zone of kimberlite generation, and ultimately be CH_4-rich. The implication is that reduced C as diamond or CH_4 in the mantle would be oxidized by ferric iron during upwelling to produce CO_2 in a manner analogous to that suggested by Taylor and Green (*4*) for melting caused by oxidation of infiltrating reduced fluids. Furthermore, because of dissolution in the garnet structure, high Fe^{3+} contents are compatible with reducing conditions and even potentially with metallic Fe at pressures on the order of 150 to 200 kbar.

The question which remains is that of carbonate [$MgCO_3$, $CaMg(CO_3)_2$] stability under these conditions (*46*). If carbonate is present together with diamond and silicates, then f_{O_2} must be

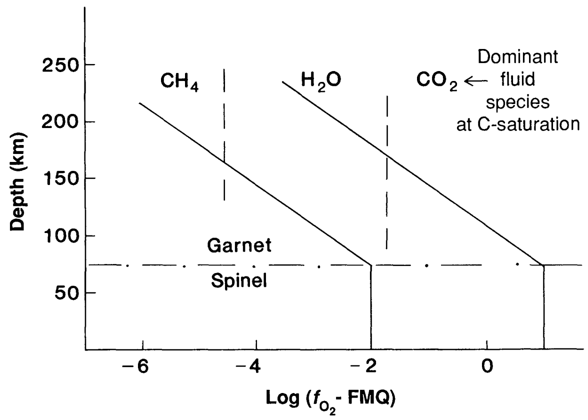

Fig. 9. Calculated effect of depth on f_{O_2} assuming that garnet is the dominant host for Fe^{3+} in the garnet peridotite field. Vertical solid lines indicate approximate range in f_{O_2} in the spinel field. Diagonal solid lines show how f_{O_2} should vary in the garnet field if the peridotites contain the same range of Fe^{3+} contents as in the spinel field. Vertical dashed lines delineate regions where CO_2, H_2O, and CH_4 are the dominant fluid species.

buffered close to FMQ (*43*) (Fig. 9). Thus, with increasing depth from the spinel field to the garnet field, the tendency of garnet to lower f_{O_2} (Fig. 9) will be buffered by reduction of carbonate to C with increasing Fe^{3+} in garnet. Only when all carbonate is exhausted will the assemblage be free to head toward low f_{O_2}. If we assume that basalts are close to CO_2 saturation in their source region with about 0.4% CO_2 by weight then the melting mantle should contain about 0.08% CO_2. Production of this amount by oxidation of diamond during ascent of a diapir requires about 0.3% additional Fe_2O_3 in peridotite in the garnet field compared to the spinel field, an amount readily accommodated by the garnet phase. It appears likely, therefore, that there is considerable interplay between the oxidation states of Fe and C in the mantle and that the mineralogic hosts of the former (garnet and spinel in particular) control fluid speciation.

Summary and Conclusions

The f_{O_2} of the asthenosphere during basalt genesis is most likely represented by the oxidation states recorded in abyssal peridotites, about +0.5 to −2.5 log units relative to FMQ. The range arises from the interplay between Fe^{3+}, reduced C (and possibly sulfur), hydrous phases, and carbonates during upwelling in the garnet and spinel peridotite fields. The decompression results in oxidation of C by Fe^{3+} to generate CO_2, together with melting of carbonate (from oxidized diamond), hydrous, and anhydrous phases. The result is to produce volatile-bearing basalts and a residuum of reduced abyssal spinel peridotites. Overall, this is a mechanism by which the mantle becomes more reduced (Fig. 9).

The average oxygen fugacity of the mantle making up the continental lithosphere is 1 log unit higher than the asthenosphere, primarily because of oxidation and hydration associated with subduction processes. Oxidation is accompanied by enrichment of large ion lithophile elements. Thus, although some continental xenoliths still show an asthenospheric or MORB-like signature, considerable heterogeneity and oxidation has occurred by secondary processes, and the subduction environment is clearly one of oxidation. In contrast to the xenoliths, larger continental massifs (Ronda, Beni Bousera) that originated in the asthenosphere and have had only short residence times in the lithosphere exhibit predominantly MORB-like oxygen fugacities.

Although we infer that oxygen fugacities are lower relative to FMQ in the garnet field than in the spinel field, this cannot be tested until appropriate oxygen barometers (reactions 2 and 3) are calibrated for garnet lherzolites and for inclusions in diamond. Because diamonds have Archaean ages, they also provide a potential source of information about any long-term changes in mantle oxidation states. Our interpretation of more reduced conditions at depth is based on the observation that Fe^{3+} readily enters the garnet structure and that Fe^{3+} garnet components have low volumes; Fe^{3+}-bearing garnet should become stable in equilibrium with iron at pressures of >150 kbar.

An extension of the crystallochemical argument is that there is no a priori reason why metallic Fe should not coexist with relatively Fe^{3+}-rich compositions like those of the upper mantle, provided there is an appropriate stable crystal structure available. In the case of the upper mantle and transition zone this is obviously the garnet structure. Equally in the lower mantle, the magnesiowustite structure would constitute a host for Fe^{3+} (*47*). Thus there is not yet any need to infer that the mantle is stratified with respect to oxidation state.

REFERENCES AND NOTES

1. E. A. Mathez, V. J. Dietrich, A. J. Irvine, *Geochim. Cosmochim. Acta* **48**, 1849 (1984).
2. J. Komprobst, F. Pireau, R. Degiovanni, J. M. Dautria, *J. Petrol.* **28**, 293 (1987).
3. A. T. Anderson, *Rev. Geophys.* **13**, 37 (1975).
4. W. R. Taylor and D. H. Green, *Nature* **332**, 349 (1988).
5. D. H. Eggler, in *Mantle Metasomatism*, M. A. Menzies and C. J. Hawkesworth, Eds. (Academic Press, London, 1987), pp. 21–41.
6. A. F. Buddington and D. H. Lindsley, *J. Petrol.* **5**, 310 (1964).
7. S. E. Haggerty, *Geophys. Res. Lett.* **5**, 443 (1978).
8. D. M. Christie, I. S. E. Carmichael, C. H. Langmuir, *Earth Planet. Sci. Lett.* **79**, 397 (1986).
9. R. O. Sack, I. S. E. Carmichael, M. L. Rivers, M. S. Ghiorso, *Contrib. Mineral. Petrol.* **75**, 369 (1980).
10. A. E. Ringwood, *Composition and Petrology of the Earth's Mantle* (McGraw-Hill, New York, 1975).
11. R. J. Arculus, J. B. Dawson, R. H. Mitchell, D. A. Gust, R. D. Holmes, *Contrib. Mineral. Petrol.* **85**, 85 (1984).
12. D. Virgo, R. W. Luth, M. A. Moats, G. C. Ulmer, *Geochim. Cosmochim. Acta* **52**, 1781 (1988).
13. H. St. C. O'Neill and V. J. Wall, *J. Petrol.* **28**, 1169 (1987).
14. H. O. A. Meyer, in *Mantle Xenoliths*, P. H. Nixon, Ed. (Wiley, New York, 1987), pp. 501–522.
15. G. S. Mattioli and B. J. Wood, *Contrib. Mineral. Petrol.* **98**, 148 (1988).
16. B. J. Wood and D. Virgo, *Geochim. Cosmochim. Acta* **53**, 1277 (1989).
17. J. Nell and B. J. Wood, *Am. Mineral.*, in press.
18. The Nell-Wood version of the spinel peridotite barometer has been parameterized in a simplified form for ease of computation. Given analyses of olivine, orthopyroxene and spinel, we obtain, compared to FMQ (*15*):

$$\log (f_{O_2})_{P,T} = \log f_{O_2}(\mathrm{FMQ})_{P,T} + \frac{220}{T} + 0.35 - \frac{0.0369P}{T}$$
$$-12 \log X_{\mathrm{Fe}}^{\mathrm{ol}} - \frac{2620}{T} X_{\mathrm{Mg}}^{\mathrm{ol}\,2} + 3 \log (X_{\mathrm{Fe}}^{\mathrm{M1}} \cdot X_{\mathrm{Fe}}^{\mathrm{M2}})^{\mathrm{opx}} + 2 \log a_{\mathrm{Fe_3O_4}}^{\mathrm{sp}}$$

where $X_{\mathrm{Fe}}^{\mathrm{ol}}$, $X_{\mathrm{Mg}}^{\mathrm{ol}}$ refer to mole fractions of Fe and Mg end-members in olivine, P is pressure in bars, T is absolute temperature, and $X_{\mathrm{Fe}}^{\mathrm{M1}}, X_{\mathrm{Fe}}^{\mathrm{M2}}$ in orthopyroxene refer to atomic fractions of Fe in the two orthopyroxene (opx) sites. These values are calculated from the analysis with the assumption of equipartition of Mg and Fe after assignment of Al^{VI}, Cr, and Ti to M1 and Ca, Na, and Mn to M2. The last term

$$\log a_{\mathrm{Fe_3O_4}}^{\mathrm{sp}} = \log \left\{ \frac{(\mathrm{Fe}^{2+}) \cdot (\mathrm{Fe}^{3+})^2}{4} \right\}$$
$$+ \frac{1}{T}[406(\mathrm{Al})^2 + 653(\mathrm{Mg})(\mathrm{Al}) + 299(\mathrm{Cr})^2 + 199(\mathrm{Al})(\mathrm{Cr}) + 346(\mathrm{Mg})(\mathrm{Cr})]$$

where bracketed terms in parentheses refer to total Mg, Cr, Al, Fe^{2+} and Fe^{3+} cations in the spinel (sp) structure on a four oxygen basis.
19. R. W. Luth, D. Virgo, F. R. Boyd, B. J. Wood, *Contrib. Mineral. Petrol.* **104**, 56 (1990).
20. P. R. A. Wells, *ibid.* **62**, 129 (1977).
21. D. H. Green and A. E. Ringwood, *Phys. Earth Planet. Inter.* **3**, 359 (1970).
22. R. A. Lange and I. S. E. Carmichael, *Geochim. Cosmochim. Acta* **51**, 2931 (1987).
23. A. F. Trial, R. L. Rudnick, L. D. Ashwal, D. J. Henry, S. C. Bergman, *Eos* **65**, 306 (1984).
24. G. S. Mattioli, M. G. Baker, M. J. Rutter, E. M. Stolper, *J. Geol.* **97**, 521 (1989).
25. P. D. Kempton, R. Harmon, H. Stosch, J. Hoefs, C. J. Hawkesworth, *Earth Planet. Sci. Lett.* **89**, 273 (1988).
26. A. M. Davis, personal communication.
27. M. F. Roden, A. J. Irvine, V. Rama Murthy, *Geochim. Cosmochim. Acta* **52**, 461 (1988).

28. A. Zindler and E. Jagoutz, *ibid.* **52**, 319 (1988).
29. J. D. Pasteris, in *Mantle Xenoliths*, P. H. Nixon, Ed. (Wiley, New York, 1987), pp. 691–707.
30. H. J. B. Dick, R. L. Fisher, W. B. Bryan, *Earth Planet. Sci. Lett.* **69**, 88 (1984).
31. L. T. Bryndzia, B. J. Wood, H. J. B. Dick, *Nature* **341**, 526 (1989).
32. Y. Bottinga and M. Javoy, *Earth Planet. Sci. Lett.* **95**, 215 (1989).
33. E. Takahashi and I. Kushiro, *Am. Mineral.* **68**, 859 (1983).
34. T. M. Gerlach and E. J. Graeber, *Nature* **313**, 273 (1985).
35. E. Stolper and J. R. Holloway, *Earth Planet. Sci. Lett.* **87**, 397 (1988).
36. F. Pileau and M. Javoy, *ibid.* **62**, 239 (1983).
37. D. J. DesMorais, *ibid.* **79**, 21 (1986).
38. A. Woodland, J. Kornprobst, B. Wood, *Geol. Soc. Am. Abstr. Progr.* **21**, A106 (1989).
39. J. Komprobst, *Contrib. Mineral. Petrol.* **23**, 283 (1969).
40. C. J. Suen and F. A. Frey, *Earth Planet. Sci. Lett.* **85**, 183 (1987).
41. P. H. Nixon, G. R. Davies, V. V. Slodkevich, S. C. Bergman, *Geol. Soc. Austr. Spec. Publ. 16*, 412 (1986).
42. J. S. Dickey, *Mineral. Soc. Am. Spec. Pap. 3*, 33 (1970).
43. D. H. Eggler, *Geophys. Res. Lett.* **10**, 365 (1983).
44. S. H. Richardson, J. J. Gurney, A. M. Erlank, J. W. Harris, *Nature* **310**, 198 (1984).
45. S. K. Saxena and Y. Fei, *Geochim. Cosmochim. Acta* **51**, 783 (1987).
46. D. H. Eggler, *Carnegie Inst. Washington Yearb.* **74**, 468 (1975).
47. J. Brynestad and H. Flood, *Z. Elektrochem.* **62**, 953 (1958).
48. This research was supported by the Gas Research Institute, contract 5089-260-1569 and the National Science Foundation.

Paleomagnetism and the Nature of the Geodynamo

R. T. MERRILL AND P. L. MCFADDEN

Records of direct observations of the earth's magnetic field cover less than a ten-millionth of the known lifetime of the field. Thus our knowledge of several geomagnetic phenomena, critical to our understanding of the geodynamo, must come from the paleomagnetic record. A combination of substantial advances during the past decade or so both in dynamo theory (previously the domain of the mathematician) and in paleomagnetism (previously the domain of the geologist) has led to provocative models of the earth's magnetic field and a better understanding of the geodynamo.

THE EARTH'S MAIN MAGNETIC FIELD IS NOW GENERALLY thought to be created by dynamo action in the earth's fluid outer core, and considerable effort has recently been devoted to obtaining useful constraints for the geodynamo problem. The areas of investigation fall into several broad categories: dynamo theory (including supercomputer simulations); predicting physical properties of the earth's interior; observations of magnetic fields in other planets and the sun; historical observations of the main field; and paleomagnetic observations. In this article we focus on some of the major areas where paleomagnetism is playing an important role in improving our understanding of the origin of the geomagnetic field. As such, it is only possible to provide a restricted view, and we have chosen to emphasize those areas associated with reversals of the field. This approach also dictates that only the briefest of comments be made on the areas other than paleomagnetism.

General Background

Not surprisingly, an analogy has been made (*1*) between the weather, largely determined by thermally driven fluid motions in the atmosphere, and the magnetic field. For example, phenomena such as fluid eddies, planetary (Rossby) waves, and thermal winds are invoked to account for various observations in both regimes. The large variation in the boundary conditions at the earth's surface significantly affects the earth's meteorology; similarly, horizontal variations at the core-mantle boundary, perhaps second only to the diversity at the earth's surface (*2*), almost certainly have a significant effect on the earth's magnetic field. Of course, the earth's two largest fluid bodies have important differences, but the analogy is sufficient to indicate that it is a formidable task to model the geodynamo. Moreover, although the atmosphere can be observed directly, the physical properties of the outer core, its boundary conditions, and its internal motions producing the magnetic field can only be inferred indirectly.

A complete mathematical solution to the geodynamo problem must simultaneously satisfy Ohm's law, the Maxwell, Navier-Stokes, Poisson, continuity, and generalized heat equations, together with the equation of state for the outer core and the appropriate boundary conditions (*3*). Most of these are partial differential equations; they are coupled; and there are strong nonlinearities. Solution would present an enormous problem even if the equation of state and boundary conditions were well known, but they are not. Because of the complexity of the problem, there are numerous partial models, each of which incorporates simplifying assumptions and restrictions and many of which use poorly known parameters.

Dynamo theory (*4*) weathered an early setback in the form of Cowling's theorem (*3, 4*) (which effectively states that axisymmetric magnetic fields of any sort cannot be maintained by dynamo action) and consequent fears that there was a general antidynamo theorem. It is now recognized that the geomagnetic field departs significantly from axial symmetry and that a magnetic field can be generated by almost any fluid motion that is sufficiently vigorous and complicated.

The magnetic induction equation (from Maxwell's equations and Ohm's law) is central to dynamo theory:

$$\frac{\partial \mathbf{H}}{\partial t} = k\nabla^2\mathbf{H} + \nabla \times (\mathbf{U} \times \mathbf{H}) \qquad (1)$$

R. T. Merrill is in the Departments of Geophysics and Geological Sciences, University of Washington, Seattle, WA 98195. P. L. McFadden is in the Division of Geophysics, Bureau of Mineral Resources, Canberra, Australia 2601.